

Resonance-like piezoelectric electron-phonon interaction in layered structures

B. A. Glavin, V. A. Kochelap, and T. L. Linnik

V. E. Lashkarev Institute of Semiconductor Physics, Prospekt Nauki 41, Kiev 03028, Ukraine

A. J. Kent, N. M. Stanton, and M. Henini

School of Physics and Astronomy, University of Nottingham, Nottingham NG7 2RD, United Kingdom

(Received 13 June 2006; revised manuscript received 16 August 2006; published 16 October 2006)

We show that mismatch of the piezoelectric parameters between layers of multiple-quantum-well structures leads to modification of the electron-phonon interaction. In particular, short-wavelength phonons propagating perpendicular to the layers with wavevector close to $2\pi n/d$, where d is the period of the structure, induce a strong smoothly varying component of the piezo-potential. As a result, they interact efficiently with two-dimensional electrons. It is shown that this property leads to emission of collimated, quasimonochromatic beams of high-frequency acoustic phonons from hot electrons in multiple-quantum well structures. We argue that this effect is responsible for the recently reported monochromatic transverse phonon emission from optically excited GaAs/AlAs superlattices and provide additional experimental evidences of this.

DOI: [10.1103/PhysRevB.74.165317](https://doi.org/10.1103/PhysRevB.74.165317)

PACS number(s): 63.20.Kr, 63.22.+m, 73.63.Hs

I. INTRODUCTION

It is now well established that the properties of acoustic phonons in layered structures can be very different from those in bulk crystals: mismatch of the elastic properties of the layers results in formation of a folded phonon spectrum and phonon stop bands, etc. This leads to the reduction of the momentum-conservation restrictions for electron-phonon, photon-phonon, and phonon-phonon interactions. In particular, the latter two processes give rise to new physics of Raman scattering of light (see Ref. 1 for review) and lattice thermal conduction (see Ref. 2 and references therein). In contrast, modification of electron-acoustic phonon interaction in multilayered structures is believed to have a marginal effect on electron transport and relaxation phenomena due to small mismatch of elastic properties in most semiconductor multilayered systems. In this communication we show that this does not apply for piezoelectric electron-acoustic phonon interactions. We claim that in this case mismatch of the piezoparameters of the quantum-well and barrier layers is essential. This mismatch changes drastically the piezopotential of phonons propagating close to the structure axis and whose wave vector is about $2\pi n/d$, where d is the structure period. In the following, we will call such phonons *resonant*. We show that the enhanced interaction strongly affects hot-carrier relaxation in multiple-quantum-well (MQW) structures. Namely, *spontaneous* emission of collimated quasimonochromatic beams of high-frequency phonons by hot electrons becomes possible. This is in contrast with *stimulated* emission of phonons, where their monochromatic character is set due to nonlinear electron-phonon dynamics in a system with population inversion.³ We argue that recent observation of monochromatic transverse acoustic phonon emission in GaAs/AlAs multilayered structures⁴ can be attributed to the considered modification of the piezoelectric electron-phonon interaction. We report also new experimental results that support this interpretation.

II. PHONON-INDUCED PIEZOELECTRIC POTENTIAL IN MULTILAYERED STRUCTURES

To begin, we recall briefly the main features of electron-acoustic phonon interaction in solitary quantum wells (QWs) (see, for example, Ref. 5). The probability of the electron intrasubband transitions is proportional to the form factor, J , given by

$$J \sim \left| \int dz \chi^2(z) \varphi \right|^2, \quad (1)$$

where χ is the envelope wave function of the confined electron and φ is the phonon-induced perturbation potential. In a uniform medium, phonons are plane waves and the same applies to φ . Thus, $\varphi \sim \exp(iq_z z)$, where q is the phonon wave vector and the z axis is directed perpendicular to the layers. As a result, for $q_z \gg 1/d_{QW}$, where d_{QW} is the QW width, the form factor is small and electron-phonon interaction is suppressed. Interaction with phonons of large in-plane wave vectors is prohibited as well due to in-plane momentum conservation. These factors suppress interaction of electrons with high-frequency acoustic phonons. This holds for both the deformation potential and piezoelectric interaction mechanisms. In nonuniform structures, however, electron-phonon interaction can be modified significantly. Nonuniformity is especially important for the piezoelectric interaction, which has a nonlocal character. In particular, the interaction potential does not necessarily mirror the properties of the phonon-induced strain. As an example, we can highlight results on piezoelectric electron-phonon interaction in thin films.⁶ As we show below, such nonlocality strongly affects the piezoelectric interaction in multilayered systems, e.g., MQW heterostructures.

The MQW structure is shown schematically in Fig. 1. The QW and barrier width are d_{QW} and d_B , respectively, and the MQW period is $d = d_{QW} + d_B$. With no tunneling coupling between the adjacent QWs, the properties of electrons are identical to those in a solitary QW. The phonons are modified due to mismatch of the elastic properties in the QW and the bar-

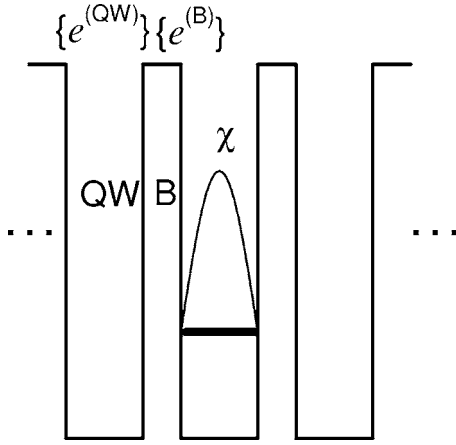


FIG. 1. Schematics of the MQW structure. Electrons are confined in QW layers with envelope wavefunction χ . The QW and barrier layers are characterized by individual values of piezoelectric parameters, $\{e^{(QW)}\}$ and $\{e^{(B)}\}$.

rier layers. However, for typical MQW structures this mismatch is small and moderate modifications are noticeable only in small regions of phonon momentum space corresponding to Bragg reflections of phonons. This has very little effect on the overall electron-phonon interaction. However, as we shall see below, mismatch of the piezoelectric parameters, while having negligible effect on the phonon mode structure, modifies the interaction potential Φ . The latter is determined by the equation

$$\nabla^2 \Phi = \frac{1}{\epsilon \epsilon_0} \nabla \cdot P. \quad (2)$$

Here ϵ is the dielectric permittivity and ϵ_0 the absolute dielectric constant. P is the polarization induced due to the piezoelectric effect: $P_i = e_{ijk} u_{jk}$, where u_{jk} is strain tensor and e_{ijk} are piezoconstants. For the case of strain induced by acoustic phonons of wave vector $q = \{q_x, q_y, q_z\}$, the potential can be expressed as $\Phi = \phi(z) \exp[i(q_x x + q_y y)]$, and the equation for ϕ is

$$\frac{d^2 \phi}{dz^2} - q_{\parallel}^2 \phi = R(z) \exp(iq_z z), \quad (3)$$

where $q_{\parallel} = \sqrt{q_x^2 + q_y^2}$, and R is a periodic function: $R(z) = R(z+d)$. The periodicity of R is due to the piezoelectric parameters mismatch in the QW and barrier layers. The specific form of R depends on the crystal structure of the materials which constitute the MQW and also the phonon wave vector and polarization. It is convenient to expand $R(z)$ as a Fourier series

$$R(z) = \sum_{n=-\infty}^{\infty} R_n \exp(iq_0 n z), \quad q_0 = 2\pi/d. \quad (4)$$

Then, the solution of Eq. (3) is

$$\phi = -\exp(iq_z z) \sum_{n=-\infty}^{\infty} \frac{R_n \exp(iq_0 n z)}{(q_z + q_0 n)^2 + q_{\parallel}^2}. \quad (5)$$

We see that for $q_z \approx -q_0 n$, the potential has a component which is a smooth function of z . As a result, the form factor for such q_z is not suppressed, even if $q_z d_{QW} \gg 1$. Furthermore, for small q_{\parallel} the amplitude of the smoothly varying component is large. Therefore, the role of mismatch of the piezoconstants is important for resonant phonons which propagate close to the MQW axis.

Particular characteristics of the piezoelectric interaction are determined by the coefficients R_n . It is convenient to present them in the following form:

$$R_0 = -q^2 \frac{e \bar{e}}{\epsilon \epsilon_0},$$

$$R_n = i \frac{e \bar{\delta e} q}{\epsilon \epsilon_0 d} [1 - \exp(-iq_0 n d_B)], \quad n \neq 0. \quad (6)$$

Here e is elementary electric charge and \bar{e} and $\bar{\delta e}$ are characteristic piezoconstants, which depend on the direction and polarization of phonon. Note that in Eq. (6) and subsequently Eq. (8) we assume that the amplitude of the displacement for a phonon is unity. We now consider in detail the example of a GaAs/AlAs MQW structure with its growth axis parallel to the (001) crystal axis. The structures are composed of cubic-symmetry materials and the piezoelectric properties are characterized by the only nonvanishing coefficient, e_{14} . Using the isotropic elastic model we obtain for longitudinal, transverse vertical, and transverse horizontal phonons the following expressions:

$$\bar{e}^{(LA)} = \frac{1}{2} \sin^2 \theta \cos \theta \sin 2\phi_{ph} \left(e_{14} + \frac{d_B}{d} \delta e_{14} \right),$$

$$\bar{\delta e}^{(LA)} = \delta e_{14} \sin^2 \theta \sin 2\phi_{ph} \left(1 + \frac{3q \cos \theta}{q_0 n} \right),$$

$$\bar{e}^{(TA,v)} = \sin \theta \cos^2 \theta \sin 2\phi_{ph} \left(e_{14} + \frac{d_B}{d} \delta e_{14} \right),$$

$$\bar{\delta e}^{(TA,v)} = \delta e_{14} \sin \theta \cos \theta \sin 2\phi_{ph} \left(1 + \frac{2q \cos \theta}{q_0 n} \right),$$

$$\bar{e}^{(TA,h)} = 2 \sin \theta \cos \theta \cos 2\phi_{ph} \left(e_{14} + \frac{d_B}{d} \delta e_{14} \right),$$

$$\bar{\delta e}^{(TA,h)} = \delta e_{14} \sin \theta \cos 2\phi_{ph} \left(1 + \frac{2q \cos \theta}{q_0 n} \right). \quad (7)$$

Here e_{14} is the piezoconstant in the QW, δe_{14} is the mismatch of the piezoconstants in the barrier and the QW, and θ , ϕ_{ph} are spherical angles of the phonon wave vector. The polarizations of transverse phonons are defined such that the displacement for the horizontally polarized phonon is parallel to the layers of the MQW, and for the vertically polarized phonon it lies in the plane formed by the wave vector and the

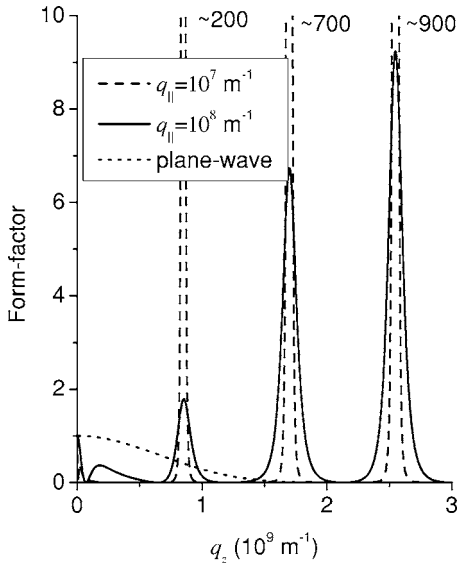


FIG. 2. Form factors of electron-phonon interaction as a function of the z component of the phonon wave vector of transverse phonons of vertical polarization for two values of the in-plane wave vector. For reference, the form factor of the plane-wave potential is provided. All form factors are normalized to its value for $q_z=0$.

normal to the layers. It is straightforward to obtain from these equations that close to resonance, $q_z = -q_0 n + \delta q_z$, $\delta q_z \ll |q_0 n|$, and for small in-plane wave vectors, the major mismatch contribution is due to the transverse phonons, whose form factors are

$$J^{(TA,h)} \approx 4 \frac{e^2 \delta e_{14}^2}{\epsilon^2 \epsilon_0^2 d^2} \sin^2 \frac{q_0 n d_B}{2} \cos^2 2\phi_{ph} \frac{q_{\parallel}^2}{(\delta q_z^2 + q_{\parallel}^2)^2},$$

$$J^{(TA,v)} \approx 4 \frac{e^2 \delta e_{14}^2}{\epsilon^2 \epsilon_0^2 d^2} \sin^2 \frac{q_0 n d_B}{2} \sin^2 2\phi_{ph} \frac{q_{\parallel}^2}{(\delta q_z^2 + q_{\parallel}^2)^2}. \quad (8)$$

As we see, the form-factor dependence on q_z has the shape of a peak. As q_{\parallel} decreases, the width of the peak decreases and its height increases. This is illustrated in Fig. 2, where we plot the form factor for transverse phonons of vertical polarization and $\phi_{ph} = \pi/4$ as a function of q_z for $q_{\parallel} = 10^7 \text{ m}^{-1}$ and 10^8 m^{-1} (all form factors are plotted for $d_{QW} = 6.2 \text{ nm}$, $d_B = 1.13 \text{ nm}$, and normalized to its value for $q_z = 0$; and the form factor of transverse phonons of horizontal polarization is similar to that of phonons of horizontal polarizations). For comparison, the form factor for a plane-wave potential is shown in the figure as well. The numbers near the peaks, corresponding to $q_{\parallel} = 10^7 \text{ m}^{-1}$, indicate the amplitudes of the peak.

It should be mentioned that the described features hold provided the number of periods in MQW structure, N , is big enough. Indeed, as can be shown from the solution of Poisson's equation for finite- N structure, the resonances are pronounced if $q_{\parallel} N d > 1$.

These properties of the form factor allow us to suggest that two dimensional (2D) hot electrons confined in the QWs of MQW structure can emit quasimonochromatic collimated beams of acoustic phonons. To prove this, we performed

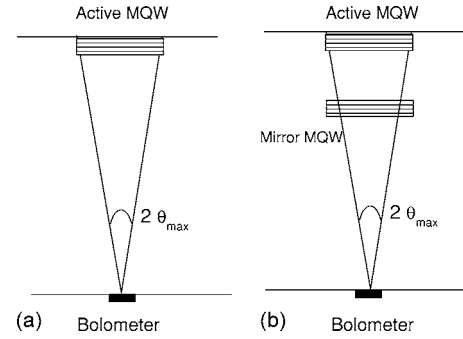


FIG. 3. (a) Schematics for measuring phonon emission from the multiple quantum well structures. The phonon signal is registered by the superconducting bolometer deposited on the back side of the substrate. (b) Similar structure but with additional filter superlattice reflecting phonons in narrow frequency bands.

calculations of the phonon emission for the experimental setup, which allows us to register the resonant phonons [see Fig. 3(a)]. In this case the emitted phonons are registered by the superconducting bolometer deposited on the back side of the substrate. Typically, the MQW and bolometer lateral dimensions are much less than the thickness of the substrate. Therefore, the bolometer probes only phonons propagating close to the MQW axis.

The results for the spectrum of the phonon emission Q are shown in Fig. 4. Q is determined as the phonon power emitted per MQW period per unit area and per unit frequency interval. The calculations were performed for a GaAs/AlAs MQW where the angle between the phonon wave vector and MQW axis is restricted by the value $\theta_{max} = 0.1$ (roughly, $2\theta_{max}$ can be estimated as the ratio of MQW lateral dimensions to the substrate thickness). We used the following material parameters: density $\rho = 5316 \text{ kg/m}^3$, longitudinal and

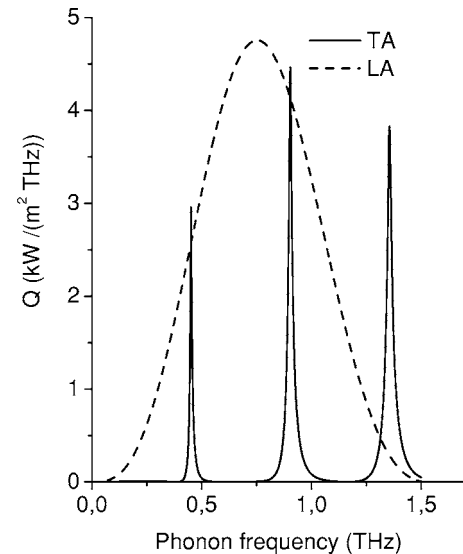


FIG. 4. The phonon emission spectrum of GaAs/AlAs MQW structure for transverse (solid line) and longitudinal (dashed line) phonons. The values of the angle between the emitted phonon wave vector and the MQW axis are restricted by $\theta_{max} = 0.1$. The electron temperature is 300 K.

transverse sound velocities $s_l=4730$ m/s, $s_t=3345$ m/s, respectively, $e_{14}=-0.16$ C/m², $\delta e_{14}=-0.065$ C/m², and $\epsilon=12.9$. These data were taken from Ref. 7. The temperature and concentration of hot electrons was assumed to be 300 K and 10^{16} m⁻², respectively, and the QW and barrier width are $d_{QW}=6.2$ nm and $d_B=1.13$ nm. The electron envelope wave functions correspond to confinement in an infinitely deep rectangular QW. The selected parameters are close to those of the experimental structure of Ref. 4, where emission of quasimonochromatic transverse phonons was detected under ultrafast laser excitation of hot carriers in GaAs/AlAs superlattice. The electron concentration and temperature are estimated based on the excitation laser wavelength and power.

As it was expected, the emission spectrum of the transverse phonons has sharp peaks for resonant phonon frequencies. For longitudinal phonons, the contribution of resonant piezoelectric interaction is very much weaker. Therefore, it cannot be resolved on the broad-spectrum deformation-potential contribution (in calculations we used the deformation potential constant 8 eV). Note that in experiments the quasimonochromatic transverse phonon signal and broad-spectrum longitudinal-phonon signal can be resolved based on the different travel times necessary to reach the bolometer.

III. COMPARISON WITH EXPERIMENTAL RESULTS

Recently, monochromatic longitudinal and transverse phonon emission was observed under the femtosecond laser excitation of electrons in GaAs/AlAs MQW.^{8,4} In these experiments the coherent nature of longitudinal phonons was detected by high-frequency modulation of the optical reflection using the pump-probe technique. Complimentary measurements of the emitted phonon spectral distribution were accomplished using the phonon filtering method. In addition to conventional structures, Fig. 2(a), “filtered” samples were manufactured, where an additional mirror superlattice was grown between the “generator” superlattice and the bolometer. The parameters of the mirror superlattice were selected such that its stop bands match the mini-Brillouin zone-center phonon frequencies of the generator superlattice. Then, the phonon signals for different excitation photon energies, below and above the fundamental edge of superlattice, were measured. In the structures without a filter, a pronounced increase of the phonon signal with increase of the photon energy was observed, which corresponds to the onset of light absorption in the superlattice. In contrast, for the filtered samples no such increase was observed for both longitudinal and transverse phonons. This suggests quasimonochromatic character of the emitted phonon spectrum. For longitudinal phonons this result can be attributed to the impulsive stimulated Raman scattering,^{9,10} which is supported by the observation of the reflectance modulation at frequency corresponding to the phonon-miniband center longitudinal phonons. However, no such modulation is present at the corresponding transverse-phonon frequency. The only remaining possibility is that monochromatic transverse phonons are emitted under the relaxation of nonequilibrium carriers following the femtosecond pulse. However, conventional

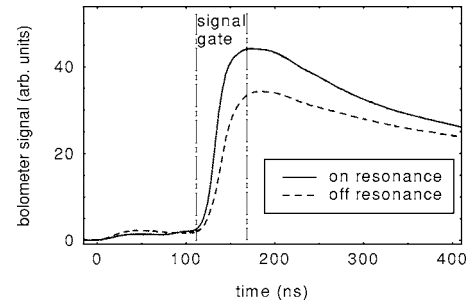


FIG. 5. Bolometer signals for on- and off-resonance optical pumping of sample A. The large peak is due to transverse phonons. The time gate used for the measurements of the angle dependence of TA intensity is indicated.

mechanisms of electron-phonon interaction do not provide such sharp phonon spectral features. We believe that the observed monochromatic transverse phonon emission could be attributed to the resonant piezoelectric-mismatch-induced interaction mechanism proposed in this paper. Note, however, that the results of the numerical calculations presented here cannot be used for quantitative estimate of the phonon emission power in these experiments. This is because of complicated relaxation pattern of electrons and holes in superlattices excited by ultrafast pulses.

The new results described here concern the angle dependence of the emission. These were obtained using the phonon imaging technique¹¹ in which the laser spot is scanned across the generator superlattice (SL), thus changing its position relative to the detector. We used two SL structures grown by MBE on 0.35-mm-thick semiinsulating GaAs substrates. Sample A contained just a generator SL and sample B contained the generator SL and a filter SL. The generator consisted of 40 periods, each of 22 monolayers (MLs) of GaAs ($d_B \approx 6.2$ nm) and 4 ML of AlAs ($d_B \approx 1.13$ nm). For these SL parameters, the first mini-Brillouin zone-center transverse acoustic (TA) phonon frequency is 450 GHz. In sample B, the notch filter was grown below the generator. It consisted of 40 periods, each of 7 ML GaAs and 7 ML AlAs ($d \approx 4$ nm), and was separated from the generator SL by a 0.5- μ m-thick GaAs spacer layer. The first mini-Brillouin zone-boundary stop band of the filter is coincident with the generator frequency and prevents 450 GHz phonons reaching the detector (bolometer) on the rear face of the substrate. Using this arrangement, we previously showed that when the generator SL was resonantly excited by 100 femtosecond laser pulses, monochromatic TA phonons of frequency 450 GHz were generated.⁴

Bolometer signals for on- and off-resonance photoexcitation of the generator SL in sample A are shown in Fig. 5. In this case the laser spot is located directly opposite the detector. The off-resonance case corresponds to the photon energy below the fundamental edge in the superlattice but above that in the bulk GaAs. Here, the bolometer response is due to ballistic and diffusive phonons generated via relaxation of the photoexcited carriers in GaAs. The on-resonance case corresponds to the photon energy above the fundamental

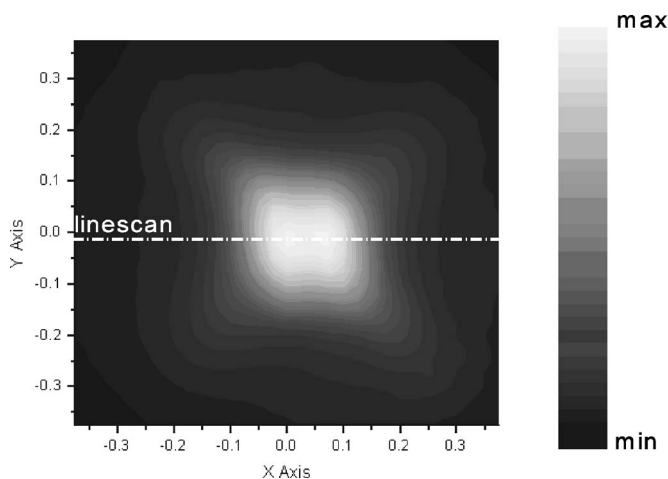


FIG. 6. Phonon image of sample B (difference between on- and off-resonance phonon intensities). The numbers indicate the position of the laser spot with respect to the bolometer in millimeters. The horizontal dashed line shows the axis of the linescans displayed in Fig. 7.

edge in the superlattice. Therefore, the increase in signal under resonant photoexcitation is due to phonon emission from carrier relaxation in the superlattice, including quasimonochromatic (450 GHz) phonons. In the angle-dependence measurements, we display the difference between the on- and off-resonance signals at times close to the ballistic time of flight for TA phonons (indicated by the dashed lines in Fig. 5). Figure 6 shows the full 2D image for sample B (filtered). The pattern is very similar to the TA phonon focusing pattern in cubic GaAs, convolved with the sizes of the laser spot (about $40\ \mu\text{m}$ diameter) and the detector ($40 \times 40\ \mu\text{m}$ squared). Linescans, taken horizontally through the center of the images (as indicated by the dashed line in Fig. 7) for samples A and B, are shown in Fig. 7 and clearly show the difference in the angle dependence of the emission. It is observed that in the case of the unfiltered sample (A) the emission is directed into a narrower range of angles. This suggests that the monochromatic (450 GHz) component of the TA signal is emitted in a direction close to the SL growth direction as predicted by the theory. Taking account of the size of the source and detector and also the phonon-focusing effects, we can estimate an upper limit for the angle to the SL normal at which the monochromatic phonons are emitted to be about 10° .

The reported experiments are for femtosecond pulsed optical excitation of the generator SL. From the above theoretical considerations it follows that quasimonochromatic trans-

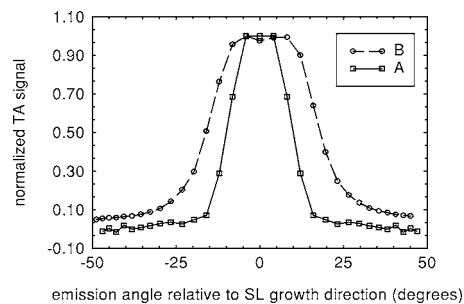


FIG. 7. Linescans of the TA intensity as a function of emission angle for samples A and B.

verse phonons can be emitted under long-pulse excitation as well. The corresponding measurements are currently in progress and they will be reported elsewhere.

IV. CONCLUSIONS

In conclusion, we have demonstrated that mismatch of the piezoelectric constants in the quantum well and barrier layers of multiple-quantum-well structures leads to resonance-like enhancement of piezoelectric electron-phonon interaction for phonons propagating close to the structure axis and having wave vectors close to $2\pi n/d$. This gives rise to the emission of quasimonochromatic phonon beams by hot electrons. We suggest that this behavior can account for the recent observation of monochromatic transverse phonon emission in GaAs/AlAs multiple-quantum-well structures. Presented in this paper, supplementary measurements of the angle dependence of the transverse phonon emission support this interpretation.

The availability of a source of monochromatic high-frequency transverse phonons can enhance the applicability of phonon-spectroscopy methods. As we have shown, the piezoelectric MQW structures are able to emit such phonons, potentially even with the use of a relatively simple laser excitation technique.

We would like to note also that the resonant contribution to piezoelectric electron-phonon interaction considered here may play an essential role in various vertical transport phenomena in semiconductor superlattice structures.

ACKNOWLEDGMENTS

This work was supported by the Royal Society of the United Kingdom. B.A.G. and V.A.K. also acknowledge partial support under the Science and Technology Center in Ukraine Grant No. 3922.

¹B. Jusserand and M. Cardona, in *Light Scattering in Solids V*, edited by M. Cardona and G. Güntherodt (Springer, Berlin, 1989).

²D. G. Cahill, W. K. Ford, K. E. Goodson, G. D. Mahan, A. Majumdar, H. J. Maris, R. Merlin, and S. R. Phillpot, *J. Appl.*

Phys. **93**, 793 (2003).

³A. J. Kent, R. N. Kini, N. M. Stanton, M. Henini, B. A. Glavin, V. A. Kochelap, and T. L. Linnik, *Phys. Rev. Lett.* **96**, 215504 (2006).

⁴N. M. Stanton, R. N. Kini, A. J. Kent, and M. Henini, *Phys. Rev.*

- B **69**, 125341 (2004).
- ⁵P. J. Price, *Solid State Commun.* **51**, 607 (1984); *Surf. Sci.* **143**, 145 (1984).
- ⁶B. A. Glavin, V. I. Pipa, V. V. Mitin, and M. A. Stroschio, *Phys. Rev. B* **65**, 205315 (2002).
- ⁷O. Madelung, *Semiconductors: Data Handbook* (Springer, Berlin, 2004).
- ⁸N. M. Stanton, R. N. Kini, A. J. Kent, M. Henini, and D. Lehmann, *Phys. Rev. B* **68**, 113302 (2003).
- ⁹R. Merlin, *Solid State Commun.* **102**, 207 (1997).
- ¹⁰T. Dekorsy, G. C. Cho, and H. Kurz, in *Light Scattering in Solids VIII*, edited by M. Cardona and G. Güntherodt (Springer, Berlin, 2000).
- ¹¹J. P. Wolfe, *Imaging Phonons: Acoustic Wave Propagation in Solids* (Cambridge University Press, Cambridge, 1998).